



Cite this: *Org. Biomol. Chem.*, 2025, **23**, 2918

## Flexible and rigid “chirally distorted” $\pi$ -systems: binaphthyl conjugates as organic CPL-active chromophores†

Giovanni Preda,<sup>a</sup> Elisa Maria Ciccarello,<sup>a</sup> Alessio Bianchi,<sup>a</sup> Francesco Zinna,<sup>b</sup> Chiara Botta,<sup>c</sup> Lorenzo Di Bari<sup>b</sup> and Dario Pasini<sup>b</sup> \*<sup>a</sup>

The inclusion of high-performance dyes into chiral  $\pi$ -conjugated systems is an effective strategy for activating significant chiroptical properties. We report the preparation and characterization of configurationally stable, axially-chiral  $\pi$ -conjugated systems in which acridone or 2,5-diarylamino-terephthalate has been fused into the chiral scaffold of a 1,1'-binaphthyl moiety. The high-yielding synthesis afforded  $\pi$ -conjugated systems with characteristics essentially matching those of the parent dyes while introducing detectable CPL activity in solution. In the acridone conjugate, good fluorescence is maintained in solution, but in the solid state, the distortion introduced by the binaphthyl system does not substantially help in restoring emissive properties; the flexibility and the emissive properties of the 2,5-diphenylamino-terephthalate chromophore are maintained in the conjugate. The new chiral chromophoric systems show absorption in the UV-vis domain, with good fluorescence properties in the visible range (quantum yields up to 23% and  $g_{lum}$  values up to  $4 \times 10^{-4}$ ).

Received 17th January 2025,  
Accepted 19th February 2025

DOI: 10.1039/d5ob00086f

rsc.li/obc

### Introduction

Chiral organic chromophores are a subject of increasing interest because they can absorb and emit polarized light, which can be measured through circular dichroism (CD) and circularly polarized luminescence (CPL) techniques, respectively. CPL can provide specific further information about the system, and CPL-active materials find potential applications in 3D displays, chiroptical materials, and optical sensors.<sup>1,2</sup>

A variety of chiral organic emitters have been proposed as CPL materials. Lanthanide-based chiral metal complexes exhibit excellent chiroptical properties and unsurpassed  $g_{lum}$  values;<sup>3</sup> however, problems associated with their strategic sourcing, use and disposal have significantly increased interest in the development of CPL-active soft organic materials. The main advantage in using organic molecules to build CPL-active systems arises from the possibility of regulating their emission in response to changes in the energy levels of their

excited states. Unlike inorganic systems, organic molecules do not yet show sufficiently high  $g_{abs}$  and  $g_{lum}$  values, so to find suitable solutions, approaches have been pursued towards unusual combinations of molecular architectures and/or their self-assembly into nanoaggregates, in order to boost CPL activity.<sup>4</sup>

Substituted 1,1'-binaphthyl derivatives are particularly interesting, in our view, for application in chiral nanomaterials, since the expression of chirality (the asymmetry induced by the stereogenic axis) is directly embedded in the two  $\pi$ -extended chromophoric regions. Their use in the field of chiroptical sensing has been recently explored, given that the conformational change in the dihedral angle defined by the two naphthyl rings occurs with an intense CD signal modulation.<sup>5</sup>

Acridone, quinacridone and their derivatives are industrially relevant dyes/pigments owing to their  $\pi$ -conjugation, internal charge transfer effects, and structural rigidity.<sup>6</sup> In fact, they are not fluorescent in the solid state because of aggregation-induced quenching effects, driven by intermolecular  $\pi$ - $\pi$  stacking and hydrogen bonding interactions.

We were thus interested in understanding whether the annulation of acridones into the  $\pi$ -extended skeleton of suitable 1,1'-binaphthyl units could impart peculiar chiroptical properties, and eventually, given the steric hindrance of the orthogonally positioned chromophores around the chiral axis, activate CPL emission. Furthermore, we envisaged to compare

<sup>a</sup>Department of Chemistry and INSTM, University of Pavia Via Taramelli 12, 27100 Pavia, Italy. E-mail: dario.pasini@unipv.it

<sup>b</sup>Dipartimento di Chimica e Chimica Industriale, Università di Pisa, Via Giuseppe Moruzzi 13, 56124 Pisa, Italy

<sup>c</sup>SCITEC-CNR, Consiglio Nazionale delle Ricerche, Istituto di Scienze e Tecnologie Chimiche ‘G. Natta’, Via A. Corti 12, 20133 Milano, Italy

† Electronic supplementary information (ESI) available. See DOI: <https://doi.org/10.1039/d5ob00086f>



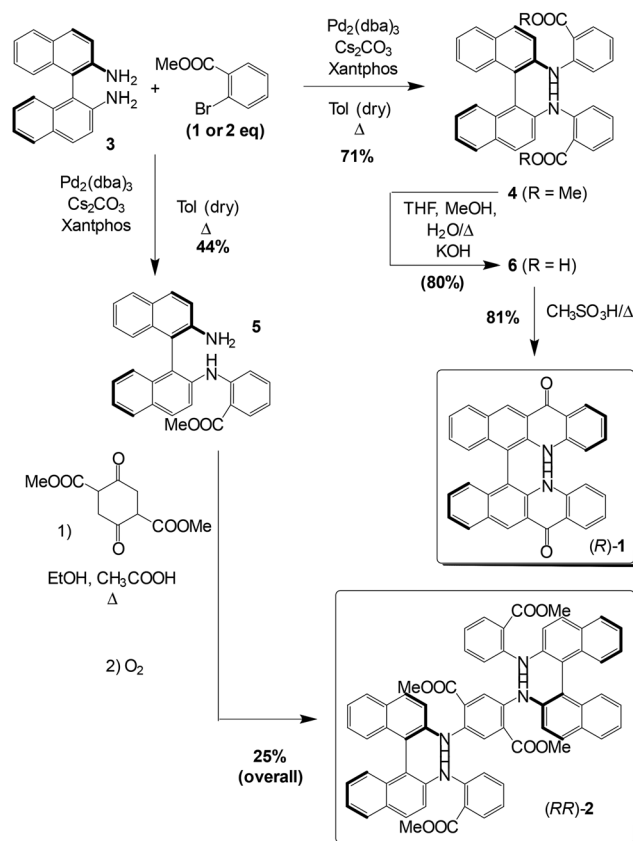
such properties with those of a recently emerged family of flexible, solid-state luminophores, 2,5-diaryl-amino-terephthalates.<sup>7</sup> They are formally obtained from quinacridones when appropriate bonds are broken, and thus their characteristic structural rigidity is lost (Fig. 1).

In this work, we efficiently fuse enantiomerically stable, substituted 1,1'-binaphthyl derivatives bearing amino functionalities at the 2,2' positions with high-performance fully organic chromophores (acridones and 2,5-diaryl-amino terephthalates). We present the solution- and solid-state (chir)optical properties of the newly synthesized compounds **1** and **2** (Fig. 1), in which the  $\pi$ -systems, while maintaining a certain degree of symmetry, are locked in a chiral environment.

## Results and discussion

### Synthetic procedures

The synthetic approach for obtaining the target compounds **1** and **2** is reported in Scheme 1. In the case of **1**, our retrosynthetic approach took advantage of the established synthesis of acridones and quinacridones, in which an arylamine substrate is functionalized with an *o*-chloro or *o*-bromo benzoate through a transition-metal mediated coupling.<sup>6</sup> As the starting point, we considered having the arylamino moiety on the binaphthyl units and thus started from enantiopure and stable (*R*-) or (*S*-)3,3'-dimethyl-[1,1'-binaphthalene]-2,2'-diamine (BINAM) **3**, since the synthesis of both enantiomers is reported in the literature. The coupling with methyl *o*-bromobenzoate was conducted through a Buchwald–Hartwig reac-



Scheme 1

tion. After the screening of reaction conditions reported in the literature, the best results were obtained using Pd(dba)<sub>3</sub> as the catalyst, Xantphos as the phosphorus-based ligand and Cs<sub>2</sub>CO<sub>3</sub> as the base. The monosubstituted and disubstituted products (*R*-)4 and (*R*-)5 could be isolated by column chromatography and obtained in 44% and 71% optimized yields, respectively.

We observed (Scheme 1) that the final cyclization step to obtain compound **1** could be conducted with higher yields when using the hydrolysed compound **6**; it was obtained in excellent yield (80%) and, since the product directly precipitates from the reaction mixture, it does not require further purification. The final cyclization to obtain (*R*-)1 proceeds *via* an intramolecular electrophilic aromatic substitution in the presence of methanesulfonic acid, which acts both as the catalyst and the reaction solvent.

The monosubstituted product (*R*-)5 (2 equiv.) was reacted with dimethyl 2,5-dioxocyclohexane-1,4-dicarboxylate, followed by molecular oxidative aromatization induced by atmospheric O<sub>2</sub> to yield (*RR*-)2. We attempted the subsequent cyclization following the synthetic sequence described for compound **1** (saponification and cyclization in the presence of methanesulfonic acid) to obtain a mixed binaphthyl-fused quinacridone and acridone system, but the desired product was detected only in trace amounts. We believe that the large conjugation of the central core could cause the insurgence of complex second-

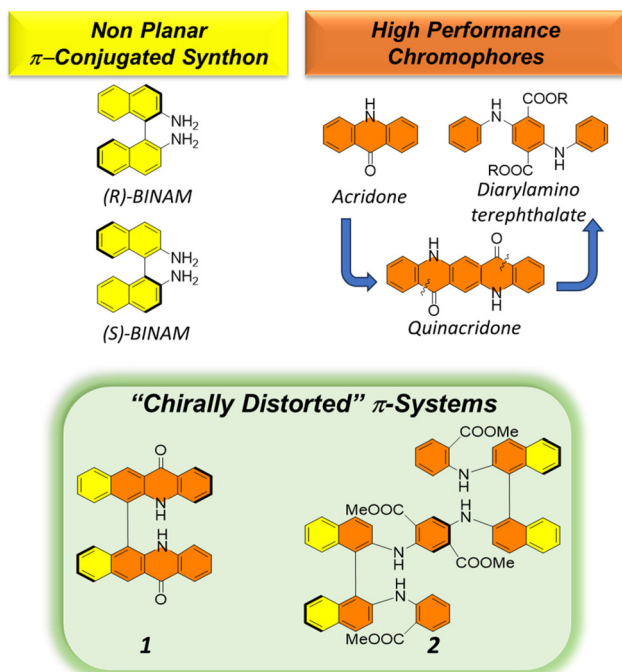


Fig. 1 Outline of the synthons that are fused to obtain flexible and rigid "chirally distorted"  $\pi$ -systems.



ary reactions in strongly acidic media, which prevented the obtainment of the desired cyclized compound. The synthetic sequences discussed above were repeated with the starting material (*S*)-BINAM, obtaining (*S*)-1 and (*SS*)-2. No racemization was observed for (*S*)-1 and even in the case of compound (*SS*)-2, bearing two binaphthyl units, as shown by chiral HPLC analysis (Fig. S1†).

### Photophysical and chiroptical characterization

Acridone is a bright yellow solid with negligible solvatochromic behaviour in solution. In a CHCl<sub>3</sub>/MeOH 1 : 1 solution, the compound shows (Fig. S2†) an intense absorption peak at 254 nm (*ca.*  $\epsilon \approx 60\,000\text{ M}^{-1}\text{ cm}^{-1}$ ) and two less intense peaks at 381 and 399 nm ( $\epsilon \approx 10\,000\text{ M}^{-1}\text{ cm}^{-1}$ ) associated with its visible HOMO–LUMO excitation (the absorption of blue-violet wavelengths gives the complementary yellow tint).

The absorption and CD spectra of compounds (*R*)-1 and (*S*)-1 in the same solvent mixture are shown in Fig. 2. The UV/vis spectrum of 1 has remarkable similarity to that of acridone, but the main peaks are shifted towards longer wavelengths, demonstrating that the annulation of an additional benzene ring into the acridone conjugated system is indeed effective in extending the conjugation and lowering the HOMO–LUMO gap (Fig. 2 top).

The  $\lambda_{\text{max}}$  were observed at 276 nm and 477 nm, with molar absorptivities almost double with respect to that of acridone (*ca.*  $100\,000$  and  $15\,000\text{ M}^{-1}\text{ cm}^{-1}$  for the two bands, respectively), in line with a compound bearing two identical acridone

chromophores. CD spectra of (*R*)-1 and (*S*)-1 revealed perfectly symmetric signatures (Fig. 2 bottom), with an exciton couplet corresponding to the main UV absorption band of the fused acridone chromophore: it is the classical CD signature of chromophores in a skewed orientation, as commonly found in atropisomeric biaryl compounds. While substantial CD activity is observed in relation to the shoulder in the UV/vis spectrum at *ca.* 300 nm, negligible CD activity could be observed corresponding to the red-shifted (477 nm) band. The maximum absorbance dissymmetry factor  $g_{\text{abs}}$  is at 305 nm with a value of  $1.27 \times 10^{-3}$  (Fig. S3†), which is in line with the majority of non-aggregated/monomeric organic compounds.

Diphenylamino dimethylterephthalate has an absorption maximum at 465 nm in CHCl<sub>3</sub> (molar absorptivity *ca.*  $10\,000\text{ M}^{-1}\text{ cm}^{-1}$ ).<sup>8</sup> The absorption and CD spectra of compounds (*RR*)-2 and (*SS*)-2 in the same solvent are shown in Fig. 3. The absorbance spectrum of 2 is not red shifted in terms of absorption maxima ( $\lambda_{\text{max}} = 466\text{ nm}$ ), indicating that the insertion of one more benzene unit into the diphenylamino dimethylterephthalate moiety does not perturb significantly the HOMO–LUMO levels; a similar molar absorptivity is detected for this band (*ca.*  $13\,000\text{ M}^{-1}\text{ cm}^{-1}$ ). The spectrum also contains other more intense bands (352 and 281 nm) related to the chromophoric units in the scaffold (including the binaphthyl units), suggesting localization rather than delocalization of the  $\pi$ -structure of the molecule. The ECD spectrum is characterized by a series of Cotton effects with alternating signs, which is strongly suggestive of a rich exciton coupling network between the manifold of electric dipole transition moments present in the complex chromophores. It is note-

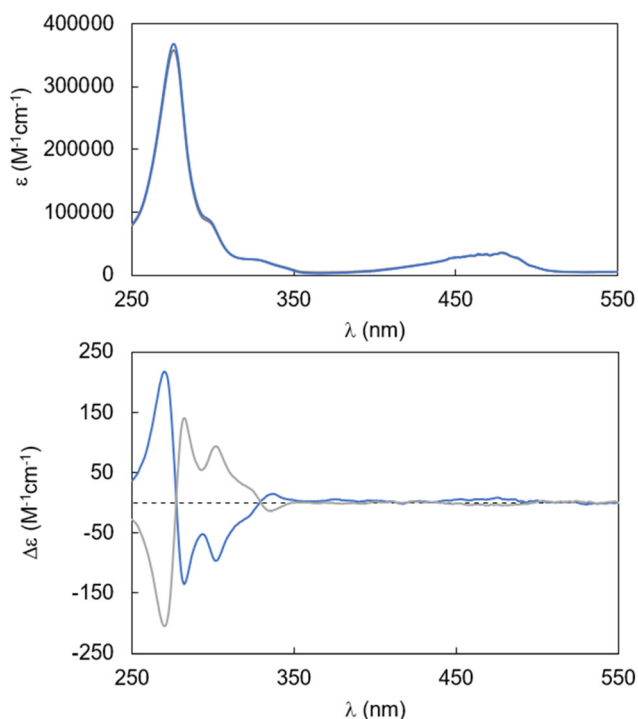


Fig. 2 UV/vis (top) and CD (bottom) spectra of compounds (*R*)-1 (blue trace) and (*S*)-1 (grey trace) in CHCl<sub>3</sub>:MeOH 1 : 1 (1.13  $\mu\text{M}$  for UV/vis, 10  $\mu\text{M}$  for CD).

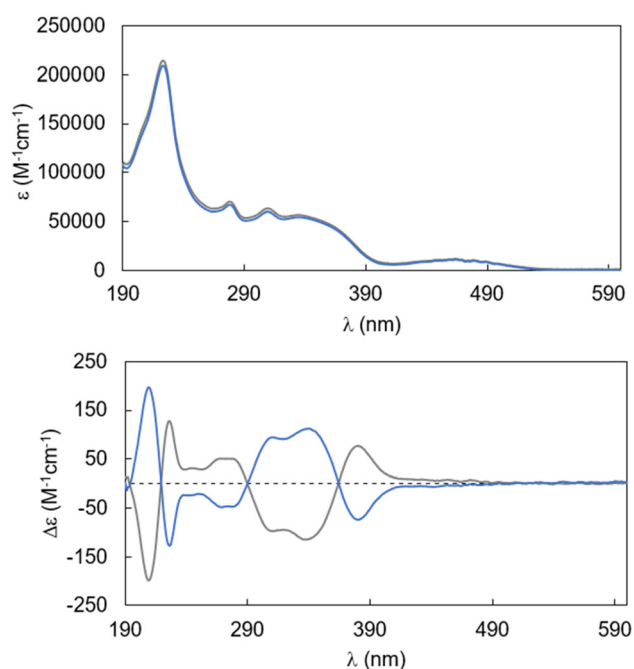


Fig. 3 Absorption and CD spectra of compounds (*RR*)-2 (blue trace) and (*SS*)-2 (grey trace) in CHCl<sub>3</sub> (27.1  $\mu\text{M}$  for UV, 26.6  $\mu\text{M}$  for CD).



worthy that, similarly to that of the enantiomers of **1**, the ECD activity related to the HOMO–LUMO transition is weak. The absorbance maximum dissymmetry factor  $g_{\text{abs}}$  is found at 390 nm with a value of  $3 \times 10^{-3}$  (Fig. S4†).

For compounds **1** and **2**, fluorescence properties in solution and in the solid state were also analyzed. In the case of **1**, a rather narrow emission band with a small Stokes shift (<50 nm) was recorded, as expected on account of its rigid structure (Fig. S5†); in compound **2**, however, intense orange fluorescence was evident even when a solution of the molecule was evaporated from MeOH, EtOH or CHCl<sub>3</sub> to form a thin film (Fig. S6†). Compound **2** in solution shows a broad emission band, compatible with a more flexible structure with substantial degrees of conformational freedom (Fig. S7†), and a large Stokes shift was observed (104 nm).

Fluorescence quantum yields in solution and in films were determined for both enantiomers of **1** and **2** (Table 1 and Fig. S8–S13†). In the case of **1**, the good luminescence performance of the parent acridone dye in solution was confirmed (quantum yield of 23% in both cases). In the solid state the fluorescence is strongly quenched: the introduction of chirality and steric hindrance protecting the acridone moiety does not substantially reduce the aggregation-induced quenching, probably due to strong intermolecular hydrogen bonding. Indeed, the FTIR spectra of **1** (Fig. S14†) are compatible with hydrogen-bonded NH stretching resonances, and are very similar to those of acridone in the solid state.<sup>9</sup> Lifetimes and monoexponential decays of the fluorescence in solution are, however, consistent with simple molecular decays.

Interestingly, in the case of **2**, good fluorescence quantum yields were obtained both in solution and in thin films, as previously reported for diphenylamino terephthalates as chromophores. The small difference in quantum yields in the case of the emission in the solid state between the two enantiomeric forms of **2** can be rationalized by differences in packing and orientation in the supramolecular structures obtained in the solid state.

CPL properties were also determined. The enantiomers of **1** displayed significant positive and negative signals in the visible domain (Fig. 4), with a luminescence dissymmetry factor ( $|g_{\text{lum}}|$ ) of  $4 \times 10^{-4}$  in correspondence to the emission maximum. In the case of **2**, luminescence dissymmetry factors ( $|g_{\text{lum}}|$ ) of up to  $2 \times 10^{-4}$  were detected. In both cases,  $g_{\text{lum}}$  is

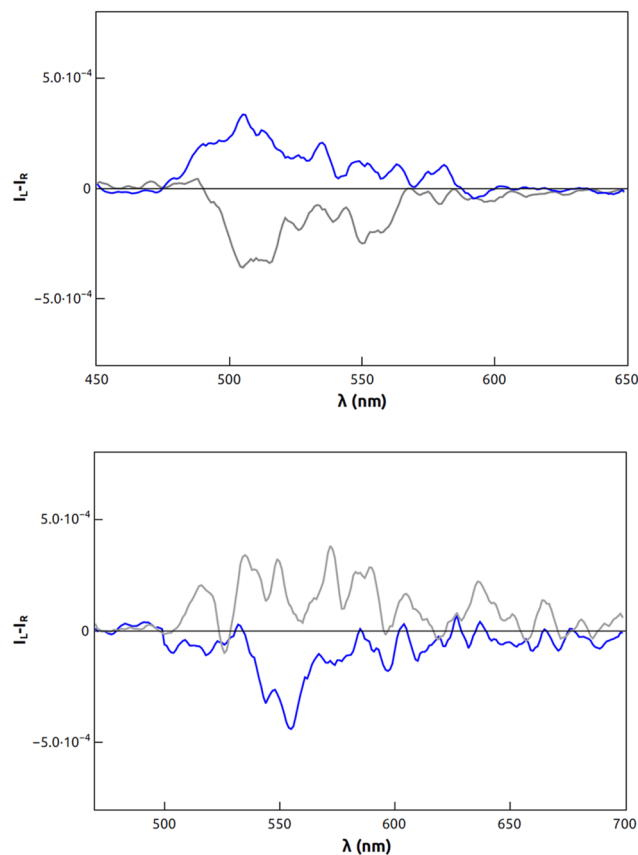


Fig. 4 CPL spectra of compounds (*R*)-**1** (blue trace) and (*S*)-**1** (grey trace) in CHCl<sub>3</sub>:MeOH 1:1 (top); (*RR*)-**2** (blue trace) and (*SS*)-**2** (grey trace) in CHCl<sub>3</sub> (bottom).

of the same order of magnitude as the corresponding  $g_{\text{abs}}$  for the HOMO–LUMO transitions; some of us have previously introduced a new quantity, named CPL brightness ( $B_{\text{CPL}}$ ), to have a complete picture of the efficiency of a CPL emitter, since dissymmetry factor ( $|g_{\text{lum}}|$ ) alone is not enough.  $B_{\text{CPL}}$  takes into account the absorption extinction coefficient and quantum yield along with ( $|g_{\text{lum}}|$ ). In the case of both **1** and **2**  $B_{\text{CPL}}$  was estimated to be  $\approx 0.5 \text{ M}^{-1} \text{ cm}^{-1}$ .<sup>10</sup> Such a value is close to the average value for the class of cationic helicenes, which are certainly more complex to achieve synthetically.<sup>10</sup>

Table 1 Photophysical properties of compounds **1** and **2** in solution (CHCl<sub>3</sub>/MeOH 1:1 and CHCl<sub>3</sub>, respectively) and as thin films from spin-coating or dropcasting from solution<sup>a</sup>

	Solution			Film		
	$\lambda_{\text{em}}$ (nm) ( $\lambda_{\text{exc}} = 488 \text{ nm}$ )	$\phi$ ( $\lambda_{\text{exc}} = 488 \text{ nm}$ )	$\tau$ (ns) ( $\lambda_{\text{exc}} = 407 \text{ nm}$ )	$\lambda_{\text{em}}$ (nm) ( $\lambda_{\text{exc}} = 407 \text{ nm}$ )	$\phi$ ( $\lambda_{\text{exc}} = 407 \text{ nm}$ )	$\tau$ (ns) ( $\lambda_{\text{exc}} = 407 \text{ nm}$ )
( <i>R</i> )- <b>1</b>	510, 540	23	7.5	544, 645	<0.1	<0.1 (407)
( <i>S</i> )- <b>1</b>	510, 540	23	7.5	544, 645	<0.1	<0.1 (407)
( <i>RR</i> )- <b>2</b>	575	11	3.2 <sup>b</sup>	583	9	1.8 <sup>b</sup> (407)
( <i>SS</i> )- <b>2</b>	575	11	3.1 <sup>b</sup>	585	12	1.8 <sup>b</sup> (407)

<sup>a</sup> See the ESI for details. <sup>†</sup> <sup>b</sup> Average lifetime  $\tau_{\text{av}}$  from 2-exponential fit.



## Conclusions

We have reported the preparation and characterization of chiral  $\pi$ -conjugated systems embedding two types of high-performance dyes with differing “flexibility” characteristics. The synthetic approach is high yielding, flexible, and potentially allows for other substituents to be incorporated into the binaphthyl skeleton.

In the acridone conjugate, good fluorescence is maintained in solution.

The flexibility and the emissive properties of the 2,5-diphenylamino-terephthalate chromophore are conserved in the conjugate, affording novel chiral dyes which are emissive both in solution and in the solid state. Compounds **2** are, to our knowledge, the first chiral versions of 2,5-diphenylamino-terephthalates utilizing the widely used and accessible binaphthyl synthons as the source of chirality. Their interesting Stokes shifts could be important in selected applications where self-absorption phenomena become an issue, such as in LSC devices.

In both cases, CPL activity in the visible region could be observed, with CPL brightness comparable to that of other, more complex, fully organic chromophores.

## Experimental

### General synthetic procedures

Commercial quinacridone was purchased from TCI (purity > 93%). (*R*)- and (*S*)-3,3'-dimethyl-[1,1'-binaphthalene]-2,2'-diamine (BINAM) **3** were prepared by Symo-Chem within the framework of a project funded by the European Consortium EUSMI. All other commercially available reagents and solvents were purchased from Sigma-Aldrich, Fluorochem, TCI and Alfa Aesar. They were all used as received. Anhydrous solvents such as THF and dichloromethane (DCM) were obtained by conventional methods through distillation with certain drying agents (Na for THF and CaH<sub>2</sub> for dichloromethane). Flash chromatography was carried out using Merck silica gel 60 (pore size 60 Å, 270–400 Mesh). <sup>1</sup>H and <sup>13</sup>C NMR spectra were recorded from solutions in deuterated solvents on 300 or 400 MHz Bruker spectrometers with the residual solvent as the internal standard. FT-IR spectra were recorded using a ThermoFisher Nicolet FT-IR spectrometer. Mass spectra of pure compounds were recorded using an Electron Spray Ionization Agilent Technologies mass spectrometer, a Direct Exposure Probe mass spectrometer and a GC-MS ThermoScientific spectrometer.

**Compound (R)-4.** Compound (*R*)-**3** (800 mg, 2.81 mmol), methyl *o*-bromobenzoate (1.30 mL, 9.28 mmol, 3.30 eq.), Cs<sub>2</sub>CO<sub>3</sub> (3.02 g, 9.28 mmol, 3.30 eq.), Pd<sub>2</sub>(dba)<sub>3</sub> (77 mg, 84.4 μmol, 0.03 eq.) and Xantphos (130.2 mg, 225 μmol, 0.08 eq.) were added to an oven-dried Schlenk tube under a nitrogen atmosphere with dry toluene (24 mL). The reaction mixture was degassed by bubbling N<sub>2</sub> for 30 minutes, then heated to reflux with stirring overnight. H<sub>2</sub>O (15 mL) was

added to the reaction mixture, the organic layer was separated and the aqueous layer was extracted with EtOAc (4 × 15 mL). The combined organic layers were dried (Na<sub>2</sub>SO<sub>4</sub>), filtered and the solvent was evaporated. The crude reaction mixture was purified by chromatography (SiO<sub>2</sub>; DCM : petroleum ether 3 : 7 to 9 : 1) to obtain the disubstituted compound (*R*)-**4** (1.1 g, 71%) and the monosubstituted product (*R*)-**5** (300 mg, 25%). Characterization for (*R*)-**4** (white solid): <sup>1</sup>H NMR (400 MHz, CDCl<sub>3</sub>) δ 8.66 (s, 1H), 7.93 (dd, *J* = 8.8 Hz, 1H), 7.89 (dd, *J* = 8.2, 1.0 Hz, 1H), 7.78 (d, *J* = 8.9 Hz, 1H), 7.72 (dd, *J* = 8.0, 1.6 Hz, 1H), 7.37 (td, *J* = 8.1, 6.6, 1.5 Hz, 2H), 7.28 (dd, *J* = 1.2 Hz, 1H), 7.25–7.19 (m, 3H), 7.11 (td, *J* = 8.6, 7.1, 1.7 Hz, 1H), 6.62 (td, *J* = 8.1, 7.1, 1.1 Hz, 1H), 3.44 (s, 3H). <sup>13</sup>C NMR (101 MHz, CDCl<sub>3</sub>) δ 167.79, 146.18, 137.83, 134.08, 133.40, 131.44, 130.61, 128.91, 128.16, 126.85, 125.01, 124.44, 123.45, 121.29, 117.71, 115.17, 113.70, 51.31. HRMS *m/z* (%) = expected: 552.1681; found 591.1648 [*M* + *K*]<sup>+</sup> (100), error –5.5 ppm.

**Compound (R)-5.** Compound (*R*)-**3** (300 mg, 1.05 mmol), methyl *o*-bromobenzoate (222 μL, 1.58 mmol, 1.50 eq.), Cs<sub>2</sub>CO<sub>3</sub> (515.6 mg, 1.58 mmol, 1.50 eq.), Pd<sub>2</sub>(dba)<sub>3</sub> (29 mg, 31.7 μmol, 0.03 eq.) and Xantphos (48.8 mg, 84.4 μmol, 0.08 eq.) were added to an oven-dried Schlenk tube under a nitrogen atmosphere with dry toluene (20 mL). The reaction mixture was degassed by bubbling N<sub>2</sub> for 30 minutes, then heated to reflux with stirring overnight. H<sub>2</sub>O (15 mL) was added to the reaction mixture, the organic layer was separated, and the aqueous layer was extracted with EtOAc (4 × 15 mL). The combined organic layers were dried (Na<sub>2</sub>SO<sub>4</sub>), filtered and the solvent was evaporated. The crude reaction mixture was purified by chromatography (SiO<sub>2</sub>; DCM : petroleum ether 3 : 7 to 9 : 1) to obtain the monosubstituted product (*R*)-**5** (192.2 mg, 44%) and the disubstituted compound (*R*)-**4** (164.4 mg, 29%). Characterization for (*R*)-**5** (white solid): <sup>1</sup>H NMR (400 MHz, CDCl<sub>3</sub>) δ 8.80–8.75 (m, 1H), 7.97 (d, *J* = 8.9 Hz, 1H), 7.92 (s, 0H), 7.90–7.78 (m, 4H), 7.47–7.38 (m, 2H), 7.36–7.15 (m, 6H), 7.09 (dd, *J* = 8.4, 1.3 Hz, 1H), 6.74 (td, *J* = 8.1, 7.0, 1.1 Hz, 1H), 3.52 (s, 3H). <sup>13</sup>C NMR (101 MHz, CDCl<sub>3</sub>) δ 167.81, 146.30, 142.51, 138.05, 133.95, 133.90, 133.67, 131.96, 130.80, 129.58, 128.93, 128.39, 128.16, 126.96, 126.76, 125.35, 124.61, 123.83, 122.99, 122.39, 121.43, 118.32, 117.96, 114.70, 113.99, 113.05, 51.50. UPLC-ESI *m/z* = 419.25 [*M* + *H*]<sup>+</sup>.

**Compound (R)-6.** Compound (*R*)-**4** (100 mg, 181 μmol) was dissolved in THF (6 mL) and MeOH (3 mL) and a solution of KOH (200 mg, 3.56 mmol) in H<sub>2</sub>O (6 mL) was added with stirring. The mixture was heated to reflux overnight. The reaction mixture was then cooled, added to H<sub>2</sub>O (100 mL) and the acidity of the solution was adjusted to pH = 2 with HCl 0.1 M to cause precipitation of the product. The solid was filtered and washed with H<sub>2</sub>O to obtain (*R*)-**6** (76 mg, 80%) as a white solid. <sup>1</sup>H NMR (200 MHz, DMSO) δ 12.76 (s, 1H), 9.35 (s, 1H), 8.26–7.52 (m, 4H), 7.50–6.49 (m, 6H).

**Compound (R)-1.** Compound (*R*)-**6** (100 mg, 191 μmol) was dissolved in methanesulfonic acid (2 mL) in an oven-dried Schlenk tube under a nitrogen atmosphere. The reaction mixture was degassed by bubbling N<sub>2</sub> for 30 minutes, then heated to reflux with stirring overnight. The mixture was



poured into a 1 : 1 mixture of ice and water (100 mL). The precipitated solid was filtered to yield pure (*R*)-1 (75 mg, 81%) as a dark red solid. <sup>1</sup>H NMR (400 MHz, DMSO) δ 9.81 (s, 1H), 9.29 (s, 1H), 8.37 (dd, *J* = 8.2, 0.9 Hz, 1H), 8.27 (dd, *J* = 8.2, 1.6 Hz, 1H), 7.58–7.39 (m, 3H), 7.31 (td, *J* = 8.8, 6.7, 1.3 Hz, 1H), 7.16 (td, *J* = 8.0, 6.7, 1.2 Hz, 1H), 6.81 (dd, *J* = 8.7, 1.0 Hz, 1H). <sup>13</sup>C NMR (101 MHz, DMSO) δ 179.13, 142.87, 138.28, 136.21, 134.36, 131.01, 129.77, 129.73, 128.82, 126.56, 124.56, 124.35, 122.52, 121.05, 119.62, 118.14, 116.16. HRMS *m/z* (%) = expected: 488.1598; found: 489.1588 [*M* + H]<sup>+</sup> (100), error –2.0 ppm. FT IR (cm<sup>-1</sup>) = 773, 1146, 1477, 1498, 1515, 2855, 2922, 3050, 3185, 3253, 3317.

**Compound (RR)-2.** Dimethyl 2,5-dioxocyclohexane-1,4-dicarboxylate (52 mg, 230 μmol, 1 eq.) was added to a solution of compound (*R*)-5 (192 mg, 459 μmol, 2 eq.) in EtOH (1.5 mL) and CH<sub>3</sub>COOH (2 mL) in an oven-dried Schlenk tube under a nitrogen atmosphere. The mixture was heated to reflux with overnight stirring. The mixture was then cooled, opened, and stirred for 3 hours without a nitrogen atmosphere, thus reducing the solvent by slow evaporation. The crude reaction mixture was purified by crystallization from DCM/EtOH/CH<sub>3</sub>COOH (6/1/1) and then by chromatography (SiO<sub>2</sub>; Hex : DCM 6 : 4) to obtain the pure product (RR)-2 (60 mg, 25% overall) as a highly fluorescent orange solid. <sup>1</sup>H NMR (400 MHz, CDCl<sub>3</sub>) δ 8.72 (s, 1H), 7.97–7.83 (m, 4H), 7.80 (d, *J* = 8.9 Hz, 1H), 7.71 (s, 1H), 7.66 (d, *J* = 8.9 Hz, 1H), 7.62 (dd, *J* = 8.0, 1.7 Hz, 1H), 7.39 (td, 1H), 7.33 (td, 1H), 7.29–7.18 (m, 5H), 7.17–7.13 (dd, 1H), 7.07 (td, *J* = 8.6, 7.1, 1.7 Hz, 1H), 6.48 (td, *J* = 8.1, 6.6, 1.4 Hz, 1H), 3.38 (s, 3H), 3.26 (s, 3H). <sup>13</sup>C NMR (101 MHz, CDCl<sub>3</sub>) δ 167.65, 166.76, 146.18, 138.59, 137.80, 136.87, 134.15, 134.09, 133.50, 131.41, 130.65, 130.07, 129.19, 128.86, 128.15, 126.93, 126.81, 125.17, 124.72, 124.52, 123.91, 123.44, 121.46, 121.22, 119.90, 119.74, 119.06, 117.66, 114.60, 113.43, 58.51, 51.50, 51.21. HRMS *m/z* (%) = expected: 1026.3701; found: 1027.3667 [*M* + H]<sup>+</sup> (100), 1049.3505 [*M* + Na]<sup>+</sup> (70), error 3.3 ppm.

### UV-vis and emission studies

UV-vis spectra were collected using a Varian Cary 50 SCAN spectrophotometer, with quartz cuvettes of an appropriate path length at 25.0 ± 0.1 °C.

The solid UV-vis diffuse reflectance spectra were recorded using a Shimadzu UV3600 spectrophotometer with BaSO<sub>4</sub> as a reference. Steady-state emission and excitation spectra and photoluminescence lifetimes were obtained using both an FLS 980 (Edinburgh Instruments Ltd) and a Nanolog (Horiba Scientific) spectrofluorometer composed of an iH320 spectrograph equipped with a Synapse QExtra charge-coupled device. The spectra were corrected for the instrument response. PL quantum yields of solutions were obtained by using rhodamine 6G as the reference. PL QYs of solid-state samples were measured with a homemade integrating sphere according to the procedure reported elsewhere.<sup>11</sup> Time-resolved TCSPC measurements were obtained with a PPD-850 single photon detector module and a DD-405L DeltaDiode Laser and analyzed with the instrument software DAS6. Decay fits were per-

formed with multi-exponential functions and average lifetimes were obtained as follows:

$$\tau_{av} = \frac{\sum_{n=1}^m B_n t_n^2}{\sum_{n=1}^m B_n t_n}$$

### CD and CPL spectroscopy

CD spectra were collected on a JASCO J1500 spectropolarimeter equipped with a Peltier temperature controller. A quartz cell of 1 cm optical path length was used for all measurements. The circularly polarized luminescence experiments for compounds *S/R*-1 and *SS/RR*-2 were carried out with a home-built CPL spectrofluoropolarimeter, in a <10<sup>-5</sup> M solution (CHCl<sub>3</sub> : MeOH 1 : 1 for *S/R*-1 and CHCl<sub>3</sub> for *SS/RR*-2). The following parameters were used: excitation: 365 nm, slit width: 5 nm, scan speed: 2 nm s<sup>-1</sup>, integration time: 2 s, PMT voltage: 450 V, accumulation: 12.<sup>9</sup>

### Author contributions

Conceptualization: G. P. and D. P.; data curation: G. P., E. M. C., A. B., C. B. and F. Z.; formal analysis: C. B. and F. Z.; funding acquisition: L. D. B. and D. P.; supervision: L. D. B. and D. P.; writing – original draft: G. P., E. M. C., A. B. and D. P.; writing – review & editing: G. P., F. Z., L. D. B., C. B. and D. P.

### Data availability

The data supporting this article have been included as part of the ESI.†

### Conflicts of interest

There are no conflicts to declare.

### Acknowledgements

We gratefully acknowledge Regione Lombardia (POR FESR 2014-2020-Call HUB Ricerca e Innovazione, Progetto 1139857 CE4WE: Circular Economy for Water and Energy) for financial support. G. P. and D. P. acknowledge support from the Ministero dell'Università e della Ricerca (MUR), the University of Pavia through the program “Dipartimenti di Eccellenza 2023–2027”, and financial support from the European Commission under the Horizon 2020 Programme by means of the grant agreement No. 200700429 EUSMI. We thank Dr Roberto Cirilli (ISS Rome) for the confirmation of the enantiomeric purity *via* chiral HPLC analysis.



## References

- (a) C. Zhang, S. Li, X. X.-Y. Dong and S.-Q. Zang, *Aggregate*, 2021, **2**, e48; (b) D.-Y. Kim, *J. Korean Phys. Soc.*, 2006, **49**, 505.
- (a) K. Yu, T. Fan, S. Lou and D. Zhang, *Prog. Mater. Sci.*, 2013, **58**, 825–873; (b) Y. Kim, B. Yeom, O. Arteaga, S. J. Yoo, S.-G. Lee, J.-G. Kim and N. A. Kotov, *Nat. Mater.*, 2016, **15**, 461–468; (c) Y. Sang, J. Han, T. Zhao, P. Duan and M. Liu, *Adv. Mater.*, 2020, **32**, 1900110; (d) L. E. MacKenzie and R. Pal, *Nat. Rev. Chem.*, 2021, **5**, 109–124; (e) R. Brandt, F. Salerno and M. J. Fuchter, *Nat. Rev. Chem.*, 2017, **1**, 0045; (f) F. Zinna, U. Giovanella and L. Di Bari, *Adv. Mater.*, 2015, **27**, 1791; (g) Y. Yang, R. C. da Costa, D.-M. Smilgies, A. J. Campbell and M. J. Fuchter, *Adv. Mater.*, 2013, **25**, 2624.
- (a) R. Carr, N. Evans and D. Parker, *Chem. Soc. Rev.*, 2012, **41**, 7673–7686; (b) Z.-L. Gong, Z.-Q. Li and Y.-W. Zhong, *Aggregate*, 2022, **3**, e177; (c) Y. Zhou, H. Li, T. Zhu, T. Gao and P. Yan, *J. Am. Chem. Soc.*, 2019, **141**, 19634.
- (a) W.-L. Zhao, M. Li, H.-Y. Lu and C.-F. Chen, *Chem. Commun.*, 2019, **55**, 13793–13803; (b) H. Oyama, M. Akiyama, K. Nakano, M. Naito, K. Nobusawa and K. Nozaki, *Org. Lett.*, 2016, **18**, 3654–3657; (c) J. Kumar, T. Nakashima and T. Kawai, *J. Phys. Chem. Lett.*, 2015, **6**, 3445–3452; (d) A. Macé, K. Hamrouni, E. S. Gauthier, M. Jean, N. Vanthuyne, L. Frédéric, G. Pieters, E. Caytan, T. Roisnel, F. Aloui, M. Srebro-Hooper, B. Carboni, F. Berrée and J. Crassous, *Chem. – Eur. J.*, 2021, **27**, 7959–7967; (e) P. M. Lorente, A. Wallabregue, F. Zinna, C. Besnard, L. Di Bari and J. Lacour, *Org. Biomol. Chem.*, 2020, **18**, 7677–7684.
- (a) P. K. Baruah, R. Gonnade, P. R. Rajamohan, H.-J. Hofmann and G. J. Sanjayan, *J. Org. Chem.*, 2007, **72**, 5077–5084; (b) L. Di Bari, G. Pescitelli and P. Salvadori, *J. Am. Chem. Soc.*, 1999, **121**, 7998–8004; (c) M. Caricato, C. Coluccini, D. Dondi, D. A. Vander Griend and D. Pasini, *Org. Biomol. Chem.*, 2010, **8**, 3272–3280; (d) M. Caricato, N. J. Leza, K. Roy, D. Dondi, G. Gattuso, L. S. Shimizu, D. A. Vander Griend and D. Pasini, *Eur. J. Org. Chem.*, 2013, 6078–6083; (e) M. Caricato, A. Olmo, C. Gargiulli, G. Gattuso and D. Pasini, *Tetrahedron*, 2012, **68**, 7861–7866; (f) M. Agnes, A. Nitti, D. A. Vander Griend, D. Dondi, D. Merli and D. Pasini, *Chem. Commun.*, 2016, **52**, 11492–11495; (g) R. Mobili, G. Preda, S. La Cognata, L. Toma, D. Pasini and V. Amendola, *Chem. Commun.*, 2022, **58**, 3897–3900; (h) D. Pasini and A. Nitti, *Chirality*, 2016, **28**, 116–123.
- (a) C. F. H. Allen and G. H. W. McKee, *Org. Synth.*, 1939, **19**, 6; (b) W. T. Wei, J.-F. Sheng, H. Miao, X. Luo, X.-H. Song, M. Yan and Y. Zou, *Adv. Synth. Catal.*, 2018, **360**, 2101–2106; (c) P. Belmont and I. Dorange, *Expert Opin. Ther. Pat.*, 2008, **18**, 1211–1224; (d) G. Preda, A. Aricò, C. Botta, D. Ravelli, D. Merli, S. Mattiello, L. Beverina and D. Pasini, *Org. Lett.*, 2023, **25**, 6490–6494.
- (a) Z. Liu, Y. Liu, F. Qi, H. Yan, Z. Jiang and Y. Chen, *Chem. – Eur. J.*, 2020, **26**, 14963–14968; (b) B. Tang, Z. Zhang, H. Liu and H. Zhang, *Chin. Chem. Lett.*, 2017, **28**, 2129–2132; (c) K. Nowak, O. Morawski, F. Zinna, G. Pescitelli, L. Di Bari, M. Górecki and M. Grzybowski, *Chem. – Eur. J.*, 2023, **29**, e202300932.
- J. H. Jin, J. M. An, D. Kim, S. Lee, M. Kim and D. Kim, *Dyes Pigm.*, 2024, **221**, 111811.
- K. V. Berezin, T. V. Krivokhizhina and V. V. Nechaev, *Opt. Spectrosc.*, 2006, **100**, 15–22.
- L. Arrico, L. Di Bari and F. Zinna, *Chem. – Eur. J.*, 2021, **27**, 2920–2934.
- J. Moreau, U. Giovanella, J.-P. Bombenger, W. Porzio, V. Vohra, L. Spadacini, G. Di Silvestro, L. Barba, G. Arrighetti, S. Destri, M. Pasini, M. Saba, F. Quochi, A. Mura, G. Bongiovanni, M. Fiorini, M. Uslenghi and C. Botta, *ChemPhysChem*, 2009, **10**, 647–653.

